Achievement of alternative configurations of vehicles on multiple lanes

Ryosuke Nishi,[1] Hiroshi Miki,[2] Akiyasu Tomoeda,[1,3] and Katsuhiro Nishinari[1,4]
[1]*Department of Aeronautics and Astronautics, Faculty of Engineering, University of Tokyo, Hongo, Bunkyo-ku, Tokyo 113-8656, Japan*
[2]*Sakura Academia Co., Hongo 3-24-17 Third Floor, Bunkyo-ku, Tokyo 113-0033, Japan*
[3]*Meiji Institute for Advanced Study of Mathematical Sciences, Meiji University, 1-1-1 Higashimita, Tamaku, Kawasaki 214-8571, Japan*
[4]*PRESTO, Japan Science and Technology Corporation, Hongo 7-3-1, Bunkyo-ku, Tokyo 113-8656, Japan*
(Received 27 October 2008; revised manuscript received 18 April 2009; published 30 June 2009)

Heavy traffic congestion occurs daily at merging sections on a highway. For relieving this congestion, possibility of alternative configuration of vehicles on multiple-lane road at a merging area is discussed in this paper. This is the configuration where no vehicles move aside on the other lane. It has merit in making a smooth merging at an intersection or a junction due to the so-called "zipper effect." We show, by developing a cellular automaton model for multiple lanes, that this configuration is achieved by simple local interactions between vehicles neighboring each other. The degree of the alternative configuration in terms of the spatial increase in parallel driving length is studied by using both numerical simulations and mean-field theory. We successfully construct a theoretical method for calculating this degree of the alternative configuration by using cluster approximation. It is shown that the theoretical results coincide with those of the simulations very well.

DOI: 10.1103/PhysRevE.79.066119 PACS number(s): 89.40.−a, 02.50.−r, 02.70.Uu, 45.70.Vn

I. INTRODUCTION

In recent years, traffic dynamics has attracted much interest of physicists, and thus it has been studied more and more diligently [1,2]. Researchers have mainly developed the analysis of the traffic flow on one-lane road by using continuous models [3] and cellular automaton (CA) models [4]. Recently, the analysis of the traffic flow on multiple-lane road at an intersection or a junction is considered as one of the important studies of traffic flow for releasing traffic congestion. Kita modeled merging interactions with game theory [5]. Hidas investigated vehicle interactions in merging and weaving by using agent based simulations [6]. Davis introduced the cooperation in merging by adding interactions between pairs of vehicles in opposite lanes [7]. He showed that velocity of vehicles in cooperative merging was higher than that in no cooperation.

However, these previous works were qualitative and did not study the configuration of vehicles in detail on two lanes before an intersection or a junction which determines the efficiency of merging. Among various configurations, the alternative configuration is the best because it realizes the smooth "zipper" merging, which is the merging of vehicles by turns on one lane and on the opposite lane. Thus, the transformation of the configuration toward the alternative configuration is significant for the improvement of the congested flow at a junction.

The purpose of this paper is to propose a simple and natural method for achievement of the alternative configuration of vehicles on two lanes. Then we study the method by both computer simulations and a mean-field theory. The communication of vehicles on two lanes is studied by the CA model which we call the multiple lanes stochastic optimal velocity (MLSOV) model. This is an extension of SOV model proposed in [8] by introducing the interactions between vehicles on the opposite lane.

This paper is organized as follows. In Sec. II we define MLSOV model, and results of simulations of two-lane flow before an intersection is presented in Sec. III. Then in Sec. IV we calculate the degree of alternative configuration by using cluster approximation and compare it with the results of the simulations. Section V is devoted to the concluding discussions.

II. MULTIPLE LANES CA MODEL WITHOUT LANE CHANGE

We propose here the MLSOV model by introducing interactions between two lanes. We choose the SOV model as a basis of our extended model because it is one of the simplest model whose fundamental diagram, i.e., flow versus density plot, shows the metastable state observed in real traffic data [8]. MLSOV model represents the interactions of vehicles on two lanes by seeing the ones on the opposite lane each other. Note that we do not take into account of the lane change behavior in this paper because we focus only on the achievement of the alternative configuration of vehicles before an intersection. In the model, the movement of all vehicles on both lane 1 and lane 2 is ruled as follows. ith vehicle on each lane moves one cell in front in one time step with probability v_i^t at time t provided that the next cell is empty. Thus the movement is described as

$$x_i^{t+1} = \begin{cases} x_i^t + 1, & \text{with probability } v_i^t \\ x_i^t, & \text{with probability } 1 - v_i^t, \end{cases} \tag{1}$$

where x_i^t is the position of ith vehicle at time t as shown in Fig. 1. v_i^t is called intension and normalized as $0 \le v_i^t \le 1$. $i+1$-th vehicle is located at the cell which is $\Delta x_{1,i}^t$ cells ahead of ith vehicle on the same lane as shown in Fig. 1. The length of one cell is set as 7.5 m.

In the MLSOV model, the time evolution of v_i^t is determined not only by ith and $i+1$-th vehicle but also $j+1$-th vehicle which is the closest vehicle to ith vehicle on the neighboring lane, with the distance $\Delta x_{2,i}^t$ cells ahead as shown in Fig. 1. v_i^t is given as

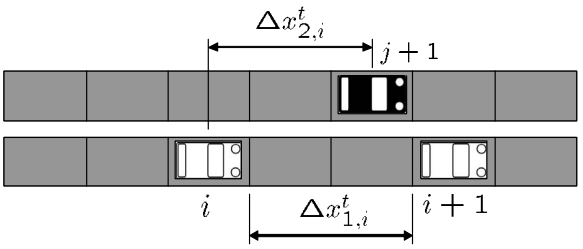

FIG. 1. The vehicles that affect the behavior of ith vehicle in MLSOV model. $i+1$-th vehicle is at the cell which is $\Delta x^t_{1,i}$ cells ahead of ith vehicle on the same lane. $j+1$-th vehicle is the closest vehicle to the ith vehicle with the distance $\Delta x^t_{2,i}$ cells ahead on the neighboring lane.

$$v_i^{t+1} - v_i^t = a\{V(\Delta x^t_{1i}, \Delta x^t_{2i}) - v_i^t\}, \tag{2}$$

where $V(\Delta x^t_{1,i}, \Delta x^t_{2,i})$ is the two-lanes optimal velocity (OV) function [3]. v_i^t tends to approach $V(\Delta x^t_{1,i}, \Delta x^t_{2,i})$ with the increase in the sensitivity parameter $a(0 \le a \le 1)$. We define for convenience $\Delta x^t_{1,i} = \infty$ in the case that $i+1$-th car does not exist and $\Delta x^t_{2,i} = \infty$ in the case that $j+1$-th car does not exist.

Now, we set the concrete form of V as

$$V(\Delta x^t_{1i}, \Delta x^t_{2i}) = \begin{cases} 0, & \Delta x^t_{1,i} = 0 \\ r, & \Delta x^t_{1,i} \ge 1 \text{ and } \Delta x^t_{2,i} = 0 \\ q, & \Delta x^t_{1,i} \ge 1 \text{ and } \Delta x^t_{2,i} = 1 \\ p, & \Delta x^t_{1,i} \ge 1 \text{ and } \Delta x^t_{2,i} \ge 2, \end{cases} \tag{3}$$

which is simple enough to achieve the alternative configuration as shown below. Here we consider special two cases of the time evolution of v_i^t with the initial condition of $v_i^0 = p$. In the case $a=0$, MLSOV model corresponds to the single-lane asymmetric simple exclusion process (ASEP) [9], since each vehicle moves irrespective of neighboring ones and v_i^t is given as

$$v_i^t = p. \tag{4}$$

In the case $a=1$, MLSOV model corresponds to a two-lane version of the zero range process (ZRP) [10], and v_i^t is given as

$$v_i^t = \begin{cases} 0, & \Delta x^t_{1,i} = 0 \\ r, & \Delta x^t_{1,i} \ge 1 \text{ and } \Delta x^t_{2,i} = 0 \\ q, & \Delta x^t_{1,i} \ge 1 \text{ and } \Delta x^t_{2,i} = 1 \\ p, & \Delta x^t_{1,i} \ge 1 \text{ and } \Delta x^t_{2,i} \ge 2. \end{cases} \tag{5}$$

Note that in the case $a=0$, the model is exactly solvable and we can theoretically calculate the stationary state and hence the fundamental diagram. In the case $a=1$, if we neglect the effect of the other lane, then we can also solve the model exactly.

III. SIMULATIONS

Our idea for making the traffic flow smooth is to draw the compartment line between the lanes as shown in Fig. 2. The line prohibits vehicles from changing lanes, and this will be used for communicating vehicles between lanes and expected to induce the zipper effect at the end of the line. Then, the disordered lane change at the merging area will be smooth and becomes safe.

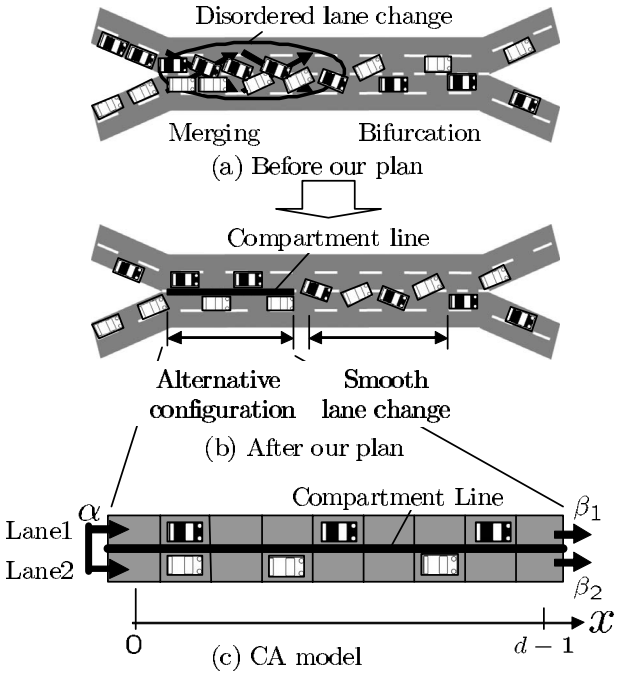

FIG. 2. (a) An example of traffic flow on a weaving section before using our plan of drawing a compartment line at the merging area. Disordered lane changes cause traffic congestion at the merging area. (b) An example of traffic flow after introducing our plan. The line prohibits vehicles from changing lanes, and is expected to make smooth lane changes by achieving alternative configurations. (c) A CA model of a two-lane road with the compartment line. Each vehicle enters in the cell at $x=0$ on both lane 1 and lane 2 simultaneously with the probability α, and goes out of the cell at $x=d-1$ with the probability $\beta_i (i=1,2)$.

The part of two-lane road indicated in Fig. 2(b) is partitioned into identical cells as shown in Fig. 2(c). The cell size is fixed and one cell can accommodate at most one vehicle. The boundaries are open, and each vehicle is updated in parallel, and it enters in the leftmost cell on lane 1 or lane 2, and moves straight ahead without changing lanes, and goes out of the rightmost cell. Although the vehicles cannot change lanes, vehicles on one lane can interact with the ones on the opposite lane by looking at the behavior of these vehicles.

All the parameters are defined in Fig. 2(c). The length of this section is d, and the leftmost cells are at $x=0$ and the rightmost cells are at $x=d-1$. In the simulations we choose the worst injection condition for merging, i.e., a vehicle enters in $x=0$ *simultaneously* on lane 1 and lane 2 with the probability α as long as *both* leftmost cells are empty. This injection is considered to be the most severe configuration for attaining the alternative configuration at the end of the road where merging occurs. If we give another condition, such that the injection into one lane is independent of the injection into another lane, the configuration is highly alternative from the beginning when the density is rather low, and

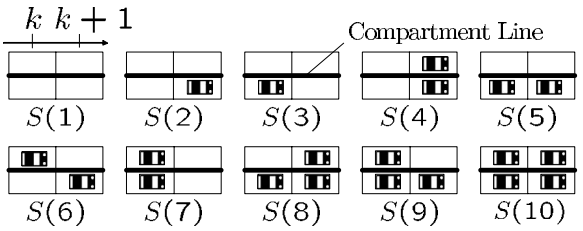

FIG. 3. Ten kinds of the state labeled by $S(n)$ in the four cells at $x=\{k,k+1\}$. The symmetry between lane 1 and lane 2 is taken into account to reduce the number of states.

vehicles do not have to synchronize with other ones on the opposite lane. Therefore, in this paper we show only the results under the simultaneous injection. We will demonstrate in the following that the alternative configuration is surely achieved in free flow region. The probability of going out of the rightmost cell of lane i is set as $\beta_i(i=1,2)$.

Next, we define two important quantities in the simulations. First, we quantify the degree of the alternative configurations of vehicles, G. G is a function of x, and $G(k)$ denotes the degree of the alternative pattern of vehicles at $x=k$. In the simulations, $G(k)$ is calculated by counting the state of the four cells at $x=\{k,k+1\}$. There are ten kinds of state labeled as $S(n)(n=1,2,\ldots 10)$ shown as Fig. 3. The symmetry between lane 1 and lane 2 is taken into account for eliminating the similar state. We defined $c(n)_k(n=1,2,\ldots 10)$ as the total number of each $S(n)$ at $x=\{k,k+1\}$ appeared through M times of simulations under the same conditions. The period for measurement of each simulation is set as $T_1 \leq t \leq T_2-1$. When there is at least one vehicle at $x=k$, the state of the four cells at $x=\{k,k+1\}$ can be $n=3,5,6,7,8,9,10$ in $S(n)$. Only $S(3)$ among them represents the perfect alternative state which is defined by Fig. 4. Thus, $G(k)$ is given by $c(n)_k$ as

$$G(k) = c(3)_k/[c(3)_k + c(5)_k + c(6)_k + c(7)_k + c(8)_k + c(9)_k + c(10)_k]. \tag{6}$$

G ranges from 0 to 1. The large value of $G(k)$ denotes that the alternative configuration of vehicles at $x=k$ is highly achieved.

Second, we define the mean intension, i.e., mean velocity on the two cells at $x=k(0\leq k\leq d-1)$ denoted by $\bar{v}(k)$, which is given by

$$\bar{v}(k) = \frac{\sum_{j=0}^{M-1}\sum_{i=0}^{N_j-1}\sum_{t=T_1}^{T_2-1} v_i^t \delta_{x_i^t,k}}{\sum_{j=0}^{M-1}\sum_{i=0}^{N_j-1}\sum_{t=T_1}^{T_2-1} \delta_{x_i^t,k}}, \tag{7}$$

where $\delta_{x_i^t,k}$ is defined as 1 if $x_i^t=k$, and 0 if $x_i^t\neq k$. This is calculated through M times of simulations under the same conditions, and $N_j(0\leq j\leq M-1)$ is the total number of vehicles entering in the leftmost cells on both lane 1 and lane 2 in jth simulation. The period for measurement of each simulation is the same as that of G.

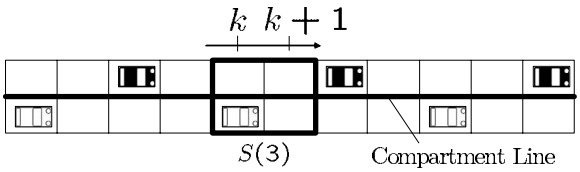

FIG. 4. The perfect alternative configuration on the two-lane road. When at least one vehicle exists at $x=k$, only $S(3)$ represents this perfect alternative configuration.

We obtained $G(x)$ versus x and $\bar{v}$ versus x by using numerical simulations. The conditions of the simulations are follows. Three sets of parameters in the OV function are chosen as $p=1$ and $(q,r)=\{(0.99,0.99),(0.8,0.8),(0.5,0.5)\}$. Moreover, four kinds of the value of the sensitivity parameter are chosen as $a=\{0.001,0.01,0.1,1\}$. The length of the road is set as $d=100$. The range of the probability of simultaneous injection on both lane 1 and lane 2 is given as $0<\alpha<0.1$. Vehicles enter in the leftmost cells with the initial intension p which appears in Eq. (3). $\beta_i(i=1,2)$ is given as each vehicle's intension v on the cell at $x=d-1$. We see that traffic flow is always in a *free flow* under this α and β_i. The number of iterations of the simulations is $M=10$, and the period for measurement is between $T_1=100\,000$ and $T_2=200\,000$. Our aim is to prevent free flow from becoming congested. Therefore, we have investigated $G(x)$ versus x and $\bar{v}$ versus x in the case of free flow, which is $\alpha<0.1$ (see Appendix A). The results show that the forms of $G(x)$ versus x, and $\bar{v}$ versus x are same in this range of α. Thus, we show only the results in the case of $\alpha=0.05$ in detail as follows.

The results of the simulations are shown in Fig. 6. From Fig. 6 we see that $G(x)$ increases monotonically from 0 to 1 as x became larger. The sharpness of the increase of $G(x)$ becomes larger as a becomes larger, and as $q(=r)$ becomes smaller from Figs. 6(a)–6(c). $\bar{v}(x)$ has one minimum value in the case of from Figs. 6(d)–6(f). The position x which gives the minimum value of $\bar{v}$ becomes smaller as a becomes larger, and as $q(=r)$ becomes smaller. The minimum value of $\bar{v}(x)$ becomes smaller as a becomes larger, and as $q(=r)$ becomes smaller.

Figures 6(a)–6(c) clearly show the achievement of the alternative configuration toward the spatial axis. These figures suggest us how we realize the smooth merging at an intersection or a junction. The sufficient length of compartment line for communicating is significant for the achievement of the alternative configurations. For instance, if we set the target G as $G_{tar}=0.6$ in the case of $a=0.01$, which are typical values of real traffic [11], and in the case of $p=1$, and $q=0.8$, then we achieve this value of G by drawing the line of 34 cell length which is equal to 255 m. Note that this alternative configuration is formed only by the local interaction within the range of $\Delta x_2\leq 1$ of each vehicle. The relationships between a and the sharpness of the increase of $G(x)$ suggest that the length of line necessary for realizing the complete alternative configuration becomes shorter if vehicles respond to the ones on the opposite lane more quickly. The relationships between q and the sharpness of the increase of $G(x)$ suggest that this length of line becomes shorter if vehicles decelerate more strongly in the case of $\Delta x_2\leq 1$.

The spatial change in $\bar{v}(x)$ is caused by the interactions between the vehicles neighboring each other in two steps. First, ith vehicle enters into $x=0$ with $\Delta x_{2,i}=0$ and slows down due to the OV function $V<1$ to apart from the ones on the neighboring lane. It keeps slowing down until $\Delta x_{2,i}\geq 2$. Then, $\Delta x_{2,i}=2$ is attained, and it starts to accelerate with $V=1$. These interactions generate the minimum value of $\bar{v}(x)$ at the point where Δx_2 of the most vehicle becomes 2. Vehicles slow down more quickly as the response parameter a becomes larger, and $q(=r)$ becomes smaller. Thus, x which give the minimum value of $\bar{v}(x)$ becomes smaller as a becomes larger, and as q becomes smaller.

Note that the hesitative behavior of drivers does not decrease the flux as long as the congestion does not grows, which is the case of $\alpha\leq 0.15$ (see Appendix A).

IV. ANALYSIS OF ALTERNATIVE CONFIGURATIONS WITH CLUSTER APPROXIMATION

In this section, we theoretically study the achievement of alternative configurations by using cluster approximation. In the approximation, the two-lane road as shown in Fig. 2 is divided into the four cells at $x=\{k,k+1\}(k=0,1,\ldots,d-2)$ which is denoted by C_k. Then, the stationary state on C_k is calculated in the order of $k=0,1,\ldots,d-2$. The state vector of C_k at time t is defined as $\Pi_k^t=\{\Pi(1)_k^t,\Pi(2)_k^t,\ldots,\Pi(10)_k^t\}$, where $\Pi(n)_k^t(1\leq n\leq 10)$ is the probability of C_k having the state S_n at time t as shown in Fig. 3. The state transition of C_k from Π_k^t to Π_k^{t+1} is defined by using the state transition matrix $\mathbf{P}_k$ whose size is 10×10. This state transition is given as

$$\Pi_k^{t+1}=\mathbf{P}_k\Pi_k^t. \tag{8}$$

The stationary state Π_k^∞ is given as the solution of

$$\Pi_k^\infty=\mathbf{P}_k\Pi_k^\infty \tag{9}$$

with the normalized condition $\Sigma_{n=1}^{10}\Pi(n)_k^\infty=1$. We construct $\mathbf{P}_k$, and calculate Π_k^∞ in the following order.

(1) We construct $\mathbf{P}_0$, and then calculate Π_0^∞.

(k) We construct $\mathbf{P}_{k-1}$, and then calculate Π_{k-1}^∞.

$$(2\leq k\leq d-2)$$

$$\vdots$$

$(d-1)$ We construct $\mathbf{P}_{d-2}$, and then calculate Π_{d-2}^∞.

This order of calculation needs approximations in constructing $\mathbf{P}_k$ $(0\leq k\leq d-3)$ because constructing $\mathbf{P}_k$ needs Π_{k+1}^∞ which is not yet calculated. The approximations for the construction of $\mathbf{P}_k$ are given in the following by the boundary conditions (BCs), and by the dynamics of vehicles on C_k.

The BCs of each $\mathbf{P}_k(k=0,1,2,\ldots,d-2)$ are given as shown in Fig. 5. The left BC of $\mathbf{P}_0$ is given strictly as vehicles entering in the leftmost cells simultaneously with probability α provided that both leftmost cells are empty. The right BC of $\mathbf{P}_0$ needs approximations because the stationary state of $C_k(1\leq k\leq d-2)$ is not yet calculated. The right BC of $\mathbf{P}_0$ is approximated as a pair of vehicles existing on both cells at $x=2$ with probability $\acute{\alpha}$. Giving $\acute{\alpha}$ simply as $\acute{\alpha}=\alpha$ is a good approximation in the case of free flow. However, giving the more accurate $\acute{\alpha}$ improves our cluster approximation because the leftmost information is important under the direction of our calculations: from left to right. Thus, we take into account the call loss at the leftmost cells in giving $\acute{\alpha}$. $\acute{\alpha}$ is given by the equation $\acute{\alpha}=\alpha(1-\acute{\alpha})$, therefore, $\acute{\alpha}=\alpha/(1+\alpha)$. The left BC of $\mathbf{P}_k(1\leq k\leq d-3)$ is the stationary state of C_{k-1} which is given strictly by Π_{k-1}^∞. The right BC of $\mathbf{P}_k(1\leq k\leq d-3)$ is the stationary state of C_{k+1} which is not yet calculated. This stationary state is approximated by using Π_{k-1}^∞ directly, i.e., the stationary state at $x=\{k+1,k+2\}$ is given by using directly that at $x=\{k-1,k\}$. The left BC of $\mathbf{P}_{d-2}$ is the stationary state of C_{d-3} which is given strictly by Π_{d-3}^∞. The right BC of $\mathbf{P}_{d-2}$ is given strictly as vehicles go out of the rightmost cell on lane $i(i=1,2)$ with probability β_i. Note that these approximations of the right BC of $P_k(0\leq k\leq d-3)$ are valid for the reason as follows. The flow considered in this paper is in free state, and the spatial change in the stationary state of the whole road is small. Therefore, approximating the right BC by using directly the left state which is already known gives a good approximated solution. Note also that in the case of free flow in ASEP, i.e., in the case of free flow, and $a=1$ of MLSOV model, the flow is controlled only by the injection condition α. This approximation to the ASEP, in which the right BC is replaced by using the left values, gives a good result which is close to the exact solution of ASEP.

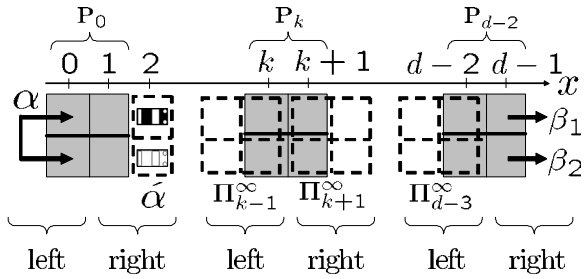

FIG. 5. The BC of each $\mathbf{P}_k(k=0,1,2,\ldots,d-2)$. The right BC of $\mathbf{P}_0$ is approximated as a pair of vehicles existing on both cells at $x=2$ with probability $\acute{\alpha}$. $\acute{\alpha}$ is approximated as $\acute{\alpha}=\alpha/(1+\alpha)$ which is the expected density of the loss system. The right BC of $\mathbf{P}_k(1\leq k\leq d-3)$ is the stationary state of C_{k+1} which is approximated by using Π_{k-1}^∞ directly. These approximations are valid as long as the flow is in free state, and the spatial change of the stationary state of the whole road is small.

The dynamics of vehicles in this cluster approximation is given as follows. We update the intension of vehicles spatially to represent the spatial change in the mean intension $\bar{v}$ observed in the simulation results [Figs. 6(d)–6(f)]. To realize the spatial change of the intension in calculating $\mathbf{P}_k$, we define $u_{i,k}(0\leq k\leq d-2)$ as the intension of ith vehicle at $k-1\leq x\leq k+1$ for $1\leq k\leq L-2$, or at $0\leq x\leq 1$ for $k=0$. To give the specific form of $u_{i,k}$, we use $\tilde{v}_k$ defined as the intension common to the vehicles at $k-1\leq x\leq k+1$ for $1\leq k\leq L-2$, or at $0\leq x\leq 1$ for $k=0$, and $\bar{V}_k(0\leq k\leq d-2)$ defined as the stationary mean OV function of C_k. $\bar{V}_k$ is calculated by using Π_k^∞ as

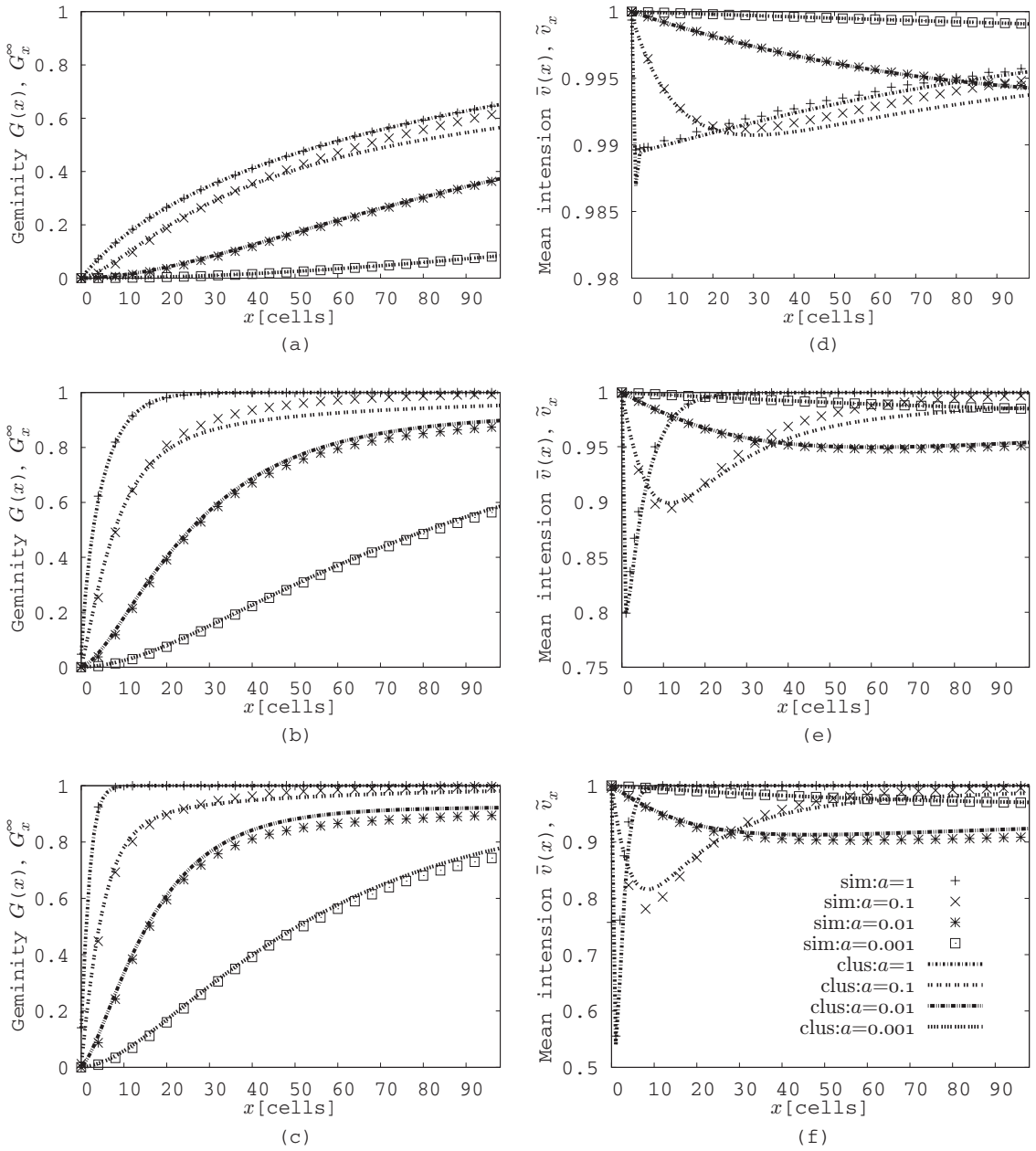

FIG. 6. $G(x)$ versus x and $\bar{v}(x)$ versus x obtained by the simulations, together with G_x^∞ versus x and $\tilde{v}_x$ versus x calculated by the four cluster approximation. G_x^∞ is defined as the degree of the alternative pattern of vehicles, and $\tilde{v}_x$ is defined as the mean intension of vehicles, which are given in the cluster approximation (see Sec. IV). $q(=r)$ is given as $q=0.99$ in the cases (a) and (d), and $q=0.8$ in the cases (b) and (e), and $q=0.5$ in the cases (c) and (f). $G(x)$ and G_x^∞ increase monotonically as x increases, and the sharpness of the increase of $G(x)$ and G_x^∞ becomes larger as a becomes larger, and as $q(=r)$ becomes smaller. $\bar{v}(x)$ and $\tilde{v}_x$ have one minimum value. The injection parameter is set as $\alpha=0.05$. For other values of α, the forms of these figures are same as long as α is small, which is the free flow case.

$$\begin{aligned}\bar{V}_k = [&p\Pi(3)_k^\infty + q\Pi(6)_k^\infty + 2r\Pi(7)_k^\infty + r\Pi(9)_k^\infty]/[\Pi(3)_k^\infty \\ &+ \Pi(5)_k^\infty + \Pi(6)_k^\infty + 2\Pi(7)_k^\infty + \Pi(8)_k^\infty + 2\Pi(9)_k^\infty \\ &+ 2\Pi(10)_k^\infty],\end{aligned} \tag{10}$$

and $\tilde{v}_k$ is updated spatially as

$$\tilde{v}_{k+1} = (1-a)\tilde{v}_k + a\bar{V}_k. \tag{11}$$

$u_{i,k}$ is given by using $\tilde{v}_k$, and by the configuration on C_k as

$$\begin{aligned}u_{i,k} &= (1-a)\tilde{v}_k + aV(\Delta x_{1,i}, \Delta x_{2,i}) \\ &= \begin{cases} (1-a)\tilde{v}_k, & \Delta x_{1,i} = 0 \\ (1-a)\tilde{v}_k + ar, & \Delta x_{1,i} \geq 1 \text{ and } \Delta x_{2,i} = 0 \\ (1-a)\tilde{v}_k + aq, & \Delta x_{1,i} \geq 1 \text{ and } \Delta x_{2,i} = 1 \\ (1-a)\tilde{v}_k + ap, & \Delta x_{1,i} \geq 1 \text{ and } \Delta x_{2,i} \geq 2. \end{cases}\end{aligned} \tag{12}$$

The detail construction of P_k is shown in Appendix A.

The degree of the alternative configurations at $x=k(0 \le k \le d-2)$ in the stationary state is defined as G_k^∞ which is given by using Π_k^∞ as

$$G_k^\infty = \Pi(3)_k^\infty / [\Pi(3)_k^\infty + \Pi(5)_k^\infty + \Pi(6)_k^\infty + \Pi(7)_k^\infty + \Pi(8)_k^\infty + \Pi(9)_k^\infty + \Pi(10)_k^\infty]. \quad (13)$$

We measure G_x^∞ versus x, and $\tilde{v}_x$ versus x, and compare them with the simulation results. The conditions of the cluster approximation are given similarly to the simulations. d, p, q, r, a, and α are the same to those of the simulations. $\beta_j(j=1,2)$ is given as the $u_{i,d-1}$ for each ith vehicle. The initial intension of vehicles is given as $\tilde{v}_0=p$. The results of the four cluster approximation are shown in Fig. 6 together with the simulation results to compare the theoretical results with the simulations.

Both G_x^∞ and $\tilde{v}_x$ coincide with $G(x)$ and $\bar{v}(x)$, respectively. The difference $|G_x^\infty - G(x)|$ is smaller in the case of $a=1$ than that of $a=0.1$. The coincidence between G_x^∞ and $G(x)$ with various a and q suggests that our four cluster approximation is a good theoretical approximation for obtaining the alternative formation. We can obtain the length of the communication line necessary for the target of G by the theoretical calculation as well as by the simulations. For other values of α, we also have obtained the same forms of G_x^∞ versus x, and $\tilde{v}_x$ versus x as long as α is small, which is the free flow case. Various G_x^∞ are generated by the spatial update of the intension as shown in Eqs. (10)–(12). $|G_x^\infty - G(x)|$ in the case of $a=1$ are smaller than that of $a=0.1$ because the calculation of $u_{i,k}$ does not contain the approximation of the spatial update of $\tilde{v}_x$ in the case of $a=1$. $u_{i,k}$ in the case of $a=1$ is given as

$$u_{i,k} = \begin{cases} 0, & \Delta x_{1i} = 0 \\ r, & \Delta x_{1i} \ge 1 \text{ and } \Delta x_{2i} = 0 \\ q, & \Delta x_{1i} \ge 1 \text{ and } \Delta x_{2i} = 1 \\ p, & \Delta x_{1i} \ge 1 \text{ and } \Delta x_{2i} \ge 2. \end{cases} \quad (14)$$

The coincidence of $\tilde{v}_x$ and $\bar{v}(x)$ suggests that this spatial update of the intension is a good approximation for expressing the spatial change of the mean intension.

V. CONCLUDING DISCUSSIONS

In this paper we have proposed a simple method for the achievement of alternative configurations of vehicles by using MLSOV model. We obtain the achievement of alternative configurations of vehicles by emergent behavior of drivers. This alternative configuration is achieved along a compartment line which is drawn between two lanes, and prohibits vehicles from changing lanes, and permits them to interact with the ones on the opposite lane. This configuration is achieved in the free flow while is not achieved in the congested flow as shown in Appendix A. This achievement is significant for traffic engineering in preventing the free flow from becoming congested by realizing the smooth "zipper merging," and is supported by the four cluster approximation. Moreover, drawing compartment lines for realizing this alternative configuration costs less than other methods for easing traffic congestion at an intersection, e.g., construction of a cubic interchange. Further improvement of the flow at an intersection or a junction by the alternative configuration, and investigating the transformation of vehicles on two lanes when the traffic flux of one lane is different from that of another lane will be published elsewhere [12].

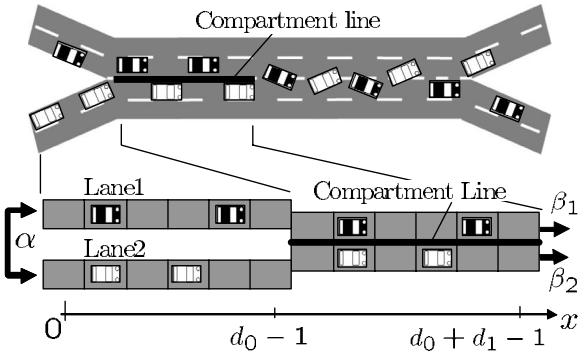

FIG. 7. A two-lane road composed of two parts partitioned into identical cells. The first part is the two-lane road before merging. Vehicles on it cannot see other vehicles on the opposite lane, and does not interact with them. The second part is the two-lane road in the merging section, and is drawn the compartment line.

APPENDIX A: THE FLUX UNDER THE HESITATIVE INTERACTIONS OF VEHICLES BETWEEN TWO LANES

In this appendix, we show the hesitative behavior used in Sec. III does not decrease the traffic flux as long as the density is low enough by using numerical simulations. We use the two-lane road model as shown in Fig. 7. This is composed of two parts. The first part is the two-lane road before merging, and vehicles on it cannot see the ones on the opposite lane, and move forward irrespective of them. This behavior is represented in MLSOV model by $\Delta x_{2,i}^t = \infty$. The second part is the two-lane road on the merging section drawn a compartment line, which is identical to the road described in Sec. II Vehicles enter in the leftmost cell of the first part on lane 1 or lane 2, and move straight ahead without changing lanes, and go out of the rightmost cell of the second part. The length of the first part is d_0, and that of the second part is d_1. The leftmost cells of the first part are set as $x=0$ and the rightmost cells of the second part are set as $x=d_0+d_1-1$. The injection condition is given similarly to that in Sec. III, i.e., a vehicle enters in $x=0$ *simultaneously* on lane 1 and lane 2 with the probability α as long as *both* leftmost cells are empty. The probability of going out of $x=d_0+d_1-1$ of lane i is set as $\beta_i(i=1,2)$.

We investigate the effect of the hesitative driver behavior on the flux of vehicles by calculating the call loss probability of the injection. It is defined as the ratio of the number of failures in simultaneous injections owing to the vehicles existing at $x=0$, to the total number of trials to enter simultaneously in $x=0$. The simulation results are shown in Fig. 8 under the conditions given in Fig. 8. The call loss probability is same irrespective of a at $\alpha < 0.15$.

This invariance of the call loss probability toward a at $\alpha < 0.15$ suggests that the hesitative behavior, represented by

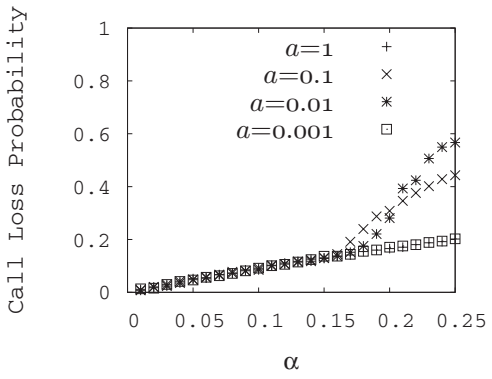

FIG. 8. Call loss probability of the injection versus α obtained by the simulations. This probability is same irrespective of the response parameter a at $\alpha<0.15$. The sharp increase in this probability in the case of $a=0.1$ and $a=0.01$ at $\alpha>0.15$ means that the congestion occurs. The parameters in the OV function are chosen as $p=1$ and $(q,r)=(0.5,0.5)$. Moreover, four kinds of the value of the sensitivity parameter are chosen as $a=\{0.001,0.01,0.1,1\}$. The length of the road is set as $d_0=d_1=100$. Vehicles enter in the leftmost cells with the initial intension p. $\beta_i(i=1,2)$ is given as each vehicle's intension v on the cell at $x=d_0+d_1-1$. The number of iterations of the simulations is $M=1$, and the period for measurement is $100\,000\leq t<200\,000$.

$p>q$ and $p>r$ in Eq. (3), does not decrease the traffic flux as long as the density is low enough. This invariance of the call loss probability also suggests that the shocks do not grow in the case of $\alpha<0.15$. Note that the sharp increase in the call loss probability in the case of $a=0.1$ and $a=0.01$ at $\alpha>0.15$ is caused by the congestion. In the case of congested flow, alternative configurations are not achieved.

We focus on preventing the free flow from becoming congested. The region of congested flow is $\alpha>0.15$. Around $\alpha=0.15$, the flow is in the state of the transition from free flow to congested flow. Therefore, we investigate and analyze the free flow in the case of $\alpha<0.1$. In the case of $\alpha<0.1$, the results obtained in Secs. III and IV, i.e., G versus x, and mean intension versus x, have the same forms. Therefore, we show one of the cases of free flow, which is $\alpha=0.05$, in Secs. III and IV.

APPENDIX B: THE DETAIL OF CONSTRUCTION OF THE STATE TRANSITION MATRIX P_k

In this appendix, we show the detail of construction of P_k by calculating an element of P_k. We define $P_k(i,j)$ $(1\leq i,\ j\leq 10)$ as the element of $\mathbf{P}_k$ at ith row, and jth column. $P_k(i,j)$ is the probability of the transition of the state from $S(j)$ to $S(i)$ on C_k. Among the elements of $\mathbf{P}_k$, here we choose to calculate $P_k(7,6)$ in the case of $1\leq k\leq d-3$. Then the other elements can be easily calculated accordingly. The transition from $S(6)$ to $S(7)$ on C_k is shown in Fig. 9(a), where $S(6)$ denotes the two states which are symmetric with each other between two lanes. In this calculation, Π_{k-1}^{∞}, and $\tilde{v}_k$ are already known. Π_{k-1}^{∞} is used for BC of C_k as follows. When the state on C_k is $S(6)$, the possible left BC of C_k, i.e., the possible states at $k-1\leq x\leq k$, are named $S_{L,k}^6(n)(n=2,5,6,9)$ as shown in Fig. 9(b). The configuration of vehicles of $S_{L,k}^6(n)$ is same as that of $S(n)$ as shown in Fig. 3. The probability of having $S_{L,k}^6(n)$ is set as $A_{L,k}^6(n)(n=2,5,6,9)$. $A_{L,k}^6(n)$ is the conditional probability among the all possible states $[S_{L,k}^6(2),S_{L,k}^6(5),S_{L,k}^6(6),S_{L,k}^6(9)]$, and is given as

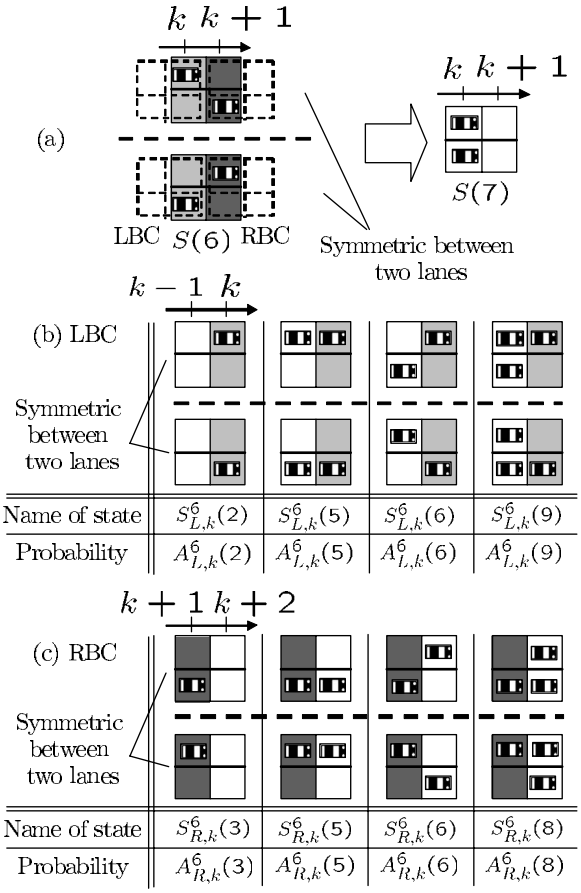

FIG. 9. (a) The transition from $S(6)$ to $S(7)$ on $C_k(1\leq k\leq d-3)$. (b) The left BC of C_k in the state of $S(6)$, and (c) the right BC of C_k in the state of $S(6)$. $A_{L,k}^6(n)(n=2,5,6,9)$ is the conditional probability of having the state $S_{L,k}^6(n)$ among the all possible states, $\{S_{L,k}^6(2),S_{L,k}^6(5),S_{L,k}^6(6),S_{L,k}^6(9)\}$. $A_{R,k}^6(m)(m=3,5,6,8)$ is the conditional probability of having the state $S_{R,k}^6(m)$ among the all possible states, $\{S_{R,k}^6(3),S_{R,k}^6(5),S_{R,k}^6(6),S_{R,k}^6(8)\}$. The right BC of C_k is given approximately by Π_{k-1}^{∞}.

$$A_{L,k}^6(n)=\frac{\Pi(n)_{k-1}^{\infty}}{\Pi(2)_{k-1}^{\infty}+\Pi(5)_{k-1}^{\infty}+\Pi(6)_{k-1}^{\infty}+\Pi(9)_{k-1}^{\infty}}. \quad \text{(B1)}$$

Note that $\Sigma_{n=2,5,6,9}A_{L,k}^6(n)=1$. When the state on C_k is $S(6)$, the possible right B.C. of C_k, i.e., the possible states at $k+1\leq x\leq k+2$, are named $S_{R,k}^6(m)(m=3,5,6,8)$ similarly to $S_{L,k}^6(n)$ as shown in Fig. 9(c). The probability of having $S_{R,k}^6(m)$ is set as $A_{R,k}^6(m)(m=3,5,6,8)$, and is given as

$$A_{R,k}^6(m)=\frac{\Pi(m)_{k-1}^{\infty}}{\Pi(3)_{k-1}^{\infty}+\Pi(5)_{k-1}^{\infty}+\Pi(6)_{k-1}^{\infty}+\Pi(8)_{k-1}^{\infty}}. \quad \text{(B2)}$$

Note that the right BC of C_k, i.e., the state at $k+1\leq x\leq k+2$ is given approximately by using Π_{k-1}^{∞}. In calculating P_k,

the intension of vehicles is determined by Eq. (12). We define $u_k^p=(1-a)\tilde{v}_k+ap$, and $u_k^q=(1-a)\tilde{v}_k+aq$, and $u_k^r=(1-a)\tilde{v}_k+ar$ for simplifying the notations. Now, we calculate $P_k(7,6)$. The transition from $S(6)$ to $S(7)$ on C_k has three stochastic processes, the movement of one vehicle from $x=k-1$ to $x=k$, and the rest of one vehicle at $x=k$, and the movement of one vehicle from $x=k$ to $x=k+1$. The probability of the first process is given by $A^6_{L,k}(6)u_k^q+A^6_{L,k}(9)u_k^r$, and the probability of the second process is given by $1-u_k^q$, and the probability of the third process is given by $A^6_{R,k}(3)u_k^p+A^6_{R,k}(6)u_k^q$. Therefore, $P_k(7,6)$ is given as

$$P_k(7,6)=[A^6_{L,k}(6)u_k^q+A^6_{L,k}(9)u_k^r](1-u_k^q)\times[A^6_{R,k}(3)u_k^p+A^6_{R,k}(6)u_k^q]. \quad \text{(B3)}$$

The other elements of $P_k(k=0,\ldots,d-2)$ under the conditions $\beta_j=u_{i,d-1}(j=1,2)$ for ith vehicle are uniquely determined similarly to $P_k(7,6)$, and are shown in [11].

[1] D. Helbing, Rev. Mod. Phys. **73**, 1067 (2001).
[2] D. Chowdhury, L. Santen, and A. Schadschneider, Phys. Rep. **329**, 199 (2000).
[3] M. Bando, K. Hasebe, A. Nakayama, A. Shibata, and Y. Sugiyama, Phys. Rev. E **51**, 1035 (1995).
[4] M. R. Evans, N. Rajewsky, and E. R. Speer, J. Stat. Phys. **95**, 45 (1999).
[5] H. Kita, Transp. Res., Part A: Policy Pract. **33**, 305 (1999).
[6] P. Hidas, Transp. Res., Part C: Emerg. Technol. **13**, 37 (2005).
[7] L. C. Davis, Physica A **361**, 606 (2006).
[8] M. Kanai, K. Nishinari, and T. Tokihiro, Phys. Rev. E **72**, 035102(R) (2005).
[9] B. Derrida, E. Domany, and D. Mukamel, J. Stat. Phys. **69**, 667 (1992).
[10] F. Spitzer, Adv. Math. **5**, 246 (1970).
[11] R. Nishi, Master's thesis, University of Tokyo, 2008.
[12] R. Nishi, H. Miki, A. Tomoeda, and K. Nishinari (unpublished).